Nuclear Inst. and Methods in Physics Research B 451 (2019) 24–26

Contents lists available at ScienceDirect

Nuclear Inst. and Methods in Physics Research B

journal homepage: www.elsevier.com/locate/nimb

# Measurements of fast neutron capture cross section for $^{180}$Hf

Fengqun Zhou[a,b,*], Yueli Song[a], Yong Li[a], Xiaojun Sun[a], Xinyi Chang[a]

[a] School of Electrical and Mechanical Engineering, Pingdingshan University, Henan Province, Pingdingshan 467000, PR China
[b] Henan Key Laboratory of Research for Central Plains Ancient Ceramics, Pingdingshan University, Henan Province, Pingdingshan 467000, PR China

ARTICLE INFO

*Keywords:*
Hafnium-180
(n,γ) reaction cross-section
Activation method
Off-line γ-ray spectrometry
Talys-1.8

ABSTRACT

The first experimental cross-section data for the $^{180}$Hf(n,γ)$^{181}$Hf reaction have been measured within the neutron energies range of 13.5–14.8 MeV using the activation technique. The fast neutrons were produced by the T(d,n)$^{4}$He reaction. Induced activities were measured by a high-resolution γ-ray spectrometer with high-purity germanium detector. The neutron fluence was determined by using the monitor reaction $^{93}$Nb(n,2n)$^{92m}$Nb. The neutron energies in the measurements were determined beforehand by the method of cross section ratios for the $^{90}$Zr(n,2n)$^{89m+g}$Zr and $^{93}$Nb(n,2n)$^{92m}$Nb reactions. The experimentally determined cross-section values were compared with the evaluation nuclear data in several major libraries of International Atomic Energy Agency and the theoretically calculated results by using the Talys1.8 code.

## 1. Introduction

The neutron induced reaction cross sections of hafnium isotopes around the neutron energy of 14 MeV are of important for the design of fusion reactor, because hafnium is a structural material of such reactor [1,2]. Among different nuclear reactions, the fast neutron capture cross section for $^{180}$Hf is of particular interest for the design of fusion reactor, and the study of the element synthesis in the astrophysics [3–5]. Since Hf is an important element in alloy materials used in the conceptual design of fusion reactor, its fast neutron capture cross section is related to neutron multiplication and the formation of radioactive nuclei and so on. In addition, the main nuclear reaction synthesis mechanism of heavy nuclides is fast neutron capture processes in nuclear astrophysics. For the $^{180}$Hf(n,γ)$^{181}$Hf reaction, we just found the cross-section experimental data of induced neutron in the 0.025 keV–3.97 MeV energy range from the International Atomic Energy Agency (IAEA) database [6]. There's a huge difference between the cross-section evaluation values of the $^{180}$Hf(n,γ)$^{181}$Hf reaction around the neutron energy of 14 MeV in several major libraries of IAEA [7]. The evaluation values of ROSFOND-2010 (Russia, 2010) [8] are much lower than those of ENDF/B-VII.0 (USA, 2006) [9], ENDF/B-VIII.0 (USA, 2018) [10], JEFF-3.3 (Europe, 2017) [11], JENDL-4.0 (Japan, 2012) [12], CENDL-3.1 (China, 2009) [13]. The evaluation data of ENDF/B-VII.0 are about twice the data of CENDL-3.1, about 4 times the data of JENDL-4.0, about 10 times the data of ENDF/B-VIII.0 and JEFF-3.3, and 1000 times more than the data of ROSFOND-2010. Thus it is necessary to measure the cross-section values of the $^{180}$Hf(n,γ)$^{181}$Hf reaction around the neutron energy of 14 MeV. In the present work, the experimental cross-section data for the $^{180}$Hf(n,γ)$^{181}$Hf reaction have been studied around the neutron energies of 13.5–14.8 MeV using the activation technique. The present results were discussed and compared with the evaluation data of ENDF/B-VII.0, ENDF/B-VIII.0, JEFF-3.3, JENDL-4.0, CENDL-3.1 and ROSFOND-2010 and the theoretically calculated results by using the Talys 1.8 code with the default parameters [14].

## 2. Experimental details

Nuclear reaction cross-section values were measured by activation and identification of the radioactive products. The details have been described in many publications [15–18]. Here we give only some salient features relevant to the present measurements.

The natural hafnium foils of 99.99% purity and 3 mm thickness were made into circular samples with a diameter of 2.0 cm. Each of them was sandwiched between two disks of thin niobium (99.99% purity and 1 mm thickness) of the same diameter, and was then wrapped in 1 mm thick cadmium foil (purity better than 99.95%).

Irradiation of the samples was carried out at the K-400 Neutron Generator at Institute of Nuclear Physics and Chemistry, China Academy of Engineering Physics. Neutrons in the 14 MeV region with a yield of about $5 \times 10^{10}$ n/s, were produced by the T(d,n)$^{4}$He reaction with a deuteron beam energy of 255 keV and a beam current of 350 μA. The solid tritium–titanium (T–Ti) target used in the generator was about 2.19 mg/cm$^2$ thick. During the irradiation, the neutron flux was monitored by the accompanying α-particles so that corrections could be

* Corresponding author.
*E-mail address:* zhoufq03@163.com (F. Zhou).

https://doi.org/10.1016/j.nimb.2019.04.084
Received 10 October 2018; Received in revised form 26 April 2019; Accepted 30 April 2019
Available online 09 May 2019
0168-583X/ 

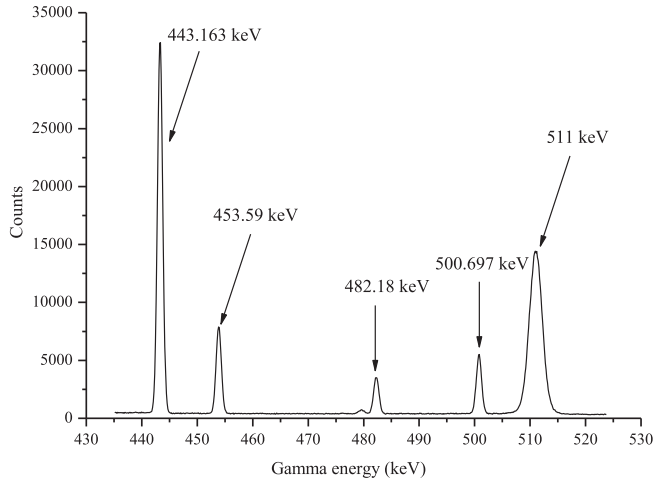


**Fig. 1.** The γ-ray spectrum of hafnium about 17 h after the end of irradiation.

**Table 1**
Reactions and associated decay data of activation products.

| Reaction | Abundance of target isotope (%) | Activation products | $T_{1/2}$ | $E_\gamma$ (keV) | $I_\gamma$ (%) |
|---|---|---|---|---|---|
| $^{180}$Hf(n,γ) | 35.08 | $^{181}$Hf | 42.39 d | 482.18 | 80.5 |
| $^{93}$Nb(n,2n) | 100[a] | $^{92m}$Nb | 10.15 d | 934.44 | 99.15 |

[a] Here, we used the value given in Ref. [21].

made for small variations in the yield. Groups of samples were placed at 0°, 45°, 90° and 135° angles relative to the deuteron beam direction. The distances of samples from the center of the T-Ti target were about 3–5 cm. The neutron energies in the measurements were determined beforehand by the method of cross section ratios for the $^{90}$Zr(n,2n)$^{89m+g}$Zr and $^{93}$Nb(n,2n)$^{92m}$Nb reactions [19].

A well-calibrated GEM-60P coaxial high-purity germanium (HPGe) detector (crystal diameter 70.1 mm, crystal length 72.3 mm) with a relative efficiency of ~68% and an energy resolution of 1.69 keV at 1.332 MeV was used to measure the γ-ray activities. The efficiency of the detector was pre-calibrated using various standard γ sources. Fig. 1 shows a typical γ-ray spectrum acquired from the hafnium samples about 17 h after the end of irradiation. The numbers of detected γ-ray counts of the reaction products were determined from their photo-peak activities after subtracting the Compton background.

The decay characteristics of the product radionuclides and the natural abundance of the target isotopes under investigation are summarized in Table 1[20]. The abundance of $^{93}$Nb came from Ref. [21] because no abundance is given in Ref. [20].

## 3. Data analysis and results

The cross-section values $\sigma_x$ of the $^{180}$Hf(n,γ)$^{181}$Hf reaction were calculated by the following equation [22]:

$$\sigma_x = \frac{[S\varepsilon I_\gamma \eta KMD]_0\,[\lambda AFC]_x}{[S\varepsilon I_\gamma \eta KMD]_x\,[\lambda AFC]_0}\sigma_0 \quad (1)$$

where $\sigma_0$ is the monitor reaction cross-section value, the subscript 0 represents the term corresponding to the monitor reaction and the subscript $x$ corresponds to the measured reaction, $\varepsilon$ is the full-energy peak (FEP) efficiency of the measured characteristic γ-ray, $I_\gamma$ is the γ-ray intensity, $\eta$ is the abundance of the target nuclide, $M$ is the mass of sample, $D = e^{-\lambda t_1} - e^{-\lambda t_2}$ is the counting collection factor, $t_1$, and $t_2$ are the time intervals from the end of the irradiation to the start and the end of counting, respectively, $A$ is the atomic weight, $C$ is the measured FEP area, λ is the decay constant, $F$ is the total correction factor of the activity:

$$F = f_s \times f_c \times f_g$$

where $f_s$, $f_c$ and $f_g$ are correction factors for the self-absorption of the sample at a given γ-energy, the coincidence sum effect of cascade γ-rays of the investigated nuclide and in the counting geometry, respectively.

$K$ is the neutron fluctuation factor:

$$K = \left[\sum_i^L \Phi_i \left(1 - e^{-\lambda \Delta t_i}\right) e^{-\lambda T_i}\right] / \Phi S$$

where $L$ is the number of time intervals into which the irradiation time is divided, $\Delta t_i$ is the duration of the $i$th time intervals, $T_i$ is the time interval from the end of the $i$th interval to the end of irradiation, $\Phi_i$ is the neutron flux averaged over the sample during $\Delta t_i$, $\Phi$ is the neutron flux averaged over the sample during the total irradiation time $T$ and $S = 1 - e^{-\lambda T}$ is the growth factor of product nuclide.

The cross-section values of the $^{180}$Hf(n,γ)$^{181}$Hf reaction were obtained relative to those of the $^{93}$Nb(n,2n)$^{92m}$Nb reaction. The cross-section values of the monitor reaction $^{93}$Nb(n,2n)$^{92m}$Nb were 457.9 ± 6.8, 459.8 ± 6.8, 459.8 ± 6.8 and 459.7 ± 5.0 mb at the neutron energies of 13.5, 14.1, 14.4 and 14.8 MeV, respectively [23]. The cross-section values measured in the present work are summarized in Table 2 and plotted in Fig. 2. Corrections were made for dead-time and pulse pile-up losses in γ-ray spectrometry, for γ-ray self-absorption in the sample, for fluctuation of the neutron flux during the irradiation and for sample geometry. The main uncertainties in our work result from the counting statistics (0.7–1.3%), the standard cross sections uncertainties (1.1–1.5%), detector efficiency (2%), the weight of samples (0.1%), the sample geometry (1%), the self-absorption of γ-ray (1.0%), and the fluctuation of the neutron flux (1%), etc.

The evaluation data of ENDF/B-VII.0, ENDF/B-VIII.0, JEFF-3.3, JENDL-4.0, CENDL-3.1, ROSFOND-2010 at the neutron energies of 13.5, 14.1, 14.4 and 14.8 MeV are also summarized in Table 2 and these evaluation curves of ENDF/B-VII.0, ENDF/B-VIII.0, JEFF-3.3, JENDL-4.0, CENDL-3.1 at the neutron energies from 0.1 to 20 MeV are plotted in Fig. 2 for comparison. When Fig. 2 is plotted, the evaluation curve of ROSFOND-2010 is not adopted because the evaluation values are very low to show clearly the relations to the other data near 14 MeV. The cross-section values of the $^{180}$Hf(n,γ)$^{181}$Hf reaction at different neutron energies from 0.1 to 20 MeV were calculated theoretically using the computer code Talys 1.8 [14]. The default values of parameters are adopted in the calculation. The theoretically calculated results are also summarized in Table 2 (in which only a few values at the neutron

**Table 2**
Summary of the cross section measurements.

| Reaction | $E_n$/MeV | σ/mb | | | | | | | |
|---|---|---|---|---|---|---|---|---|---|
| | | Present work | ENDF/B-VII.0 | ENDF/B-VIII.0 | JEFF-3.3 | JENDL-4.0 | CENDL-3.1 | ROSFOND-2010 | TALYS-1.8 |
| $^{180}$Hf(n,γ) $^{181}$Hf | 13.5 ± 0.3 | 11.9 ± 0.6 | 4.95 | 0.5094 | 0.5829 | 1.449 | 2.08 | 0.00471 | 13.4 |
| | 14.1 ± 0.2 | 11.8 ± 0.6 | 4.73 | 0.5598 | 0.5389 | 1.337 | 2.09 | 0.00404 | 12.8 |
| | 14.4 ± 0.3 | 10.4 ± 0.5 | 4.63 | 0.5792 | 0.5049 | 1.296 | 2.11 | 0.00379 | 12.5 |
| | 14.8 ± 0.2 | 12.3 ± 0.6 | 4.51 | 0.5911 | 0.4595 | 1.211 | 2.15 | 0.00349 | 12.2 |

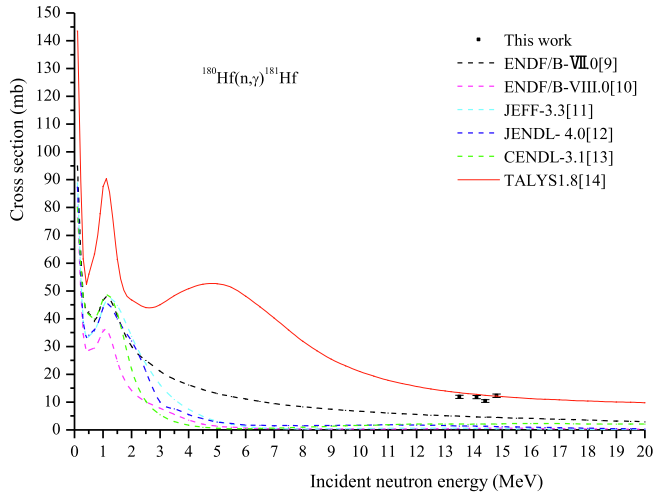


**Fig. 2.** Cross-section experimental values of the $^{180}$Hf(n,γ)$^{181}$Hf reaction within the neutron energies range of 13.5–14.8 MeV compared to the theoretical calculated data (TALYS1.8) [14] and the evaluated data from several major libraries [7].

energies of 13.5, 14.1, 14.4 and 14.8 MeV are shown) and plotted in Fig. 2 for comparison. The complete description of the Talys code can be found in the Talys1.8 manual [14].The Talys1.8 code system is able to analyze and predict nuclear reactions based on physics models and parameterizations [14,24,25]. It can calculate nuclear reactions involving neutrons, photons, protons, deuterons, tritons, $^3$He and α-particles in the 1 keV-200 MeV energy range and for target nuclides with a mass of 12 and heavier. To deal with the neutron induced reactions, the optical model is adopted. All optical model calculations are performed by ECIS-06 [26], which is implanted as a subroutine in Talys.

## 4. Discussion

The vacant target experiment should be done to subtract the influence of lower energy neutrons from the d-d reaction by accumulation of deuterium in the tritium-target with time and from background neutrons, which may originate from the scattering of thermal and epithermal neutrons from room walls etc. We didn't do vacant target experiment, but the new T-Ti target was used in present work. Furthermore, the samples were wrapped in cadmium foil and placed at the appropriate positions, which were about 3–5 cm away from the center of the T-Ti target and were far away from the walls and the upper or lower floors of the experimental hall during the irradiation. So the influence of lower energy neutrons was reduced to a very low level (negligible).

From the Table 2 and Fig. 2, we can see that the evaluation data of ROSFOND-2010 are much lower than those of ENDF/B-VII.0, ENDF/B-VIII.0, JEFF-3.3, JENDL-4.0, CENDL-3.1, the theoretically calculated results and our experimental values. The theoretically calculated data by using the Talys1.8 code are much higher than the evaluation data, whereas our experimental values are very close to the theoretical values, especially the value at 14.8 MeV neutron energy is very consistent with the theoretical value. This also means that the theoretically calculated model used to the Talys1.8 code is suitable. It should be mentioned that this work presents the first experimental cross-section data for the $^{180}$Hf(n,γ)$^{181}$Hf reaction induced by neutrons around 14 MeV.

## 5. Conclusions

We have measured the cross section data for the $^{180}$Hf(n,γ)$^{181}$Hf reaction within the neutron energies range of 13.5–14.8 MeV. Our experimental values are very close to the theoretically calculated data by using the Talys1.8 code with the default parameters. The first experimental cross-section data are expected to help new cross-section evaluations around 14 MeV neutrons for the $^{180}$Hf(n,γ)$^{181}$Hf reaction.

## Acknowledgements

We thank the crew of the K-400 Neutron Generator at Institute of Nuclear Physics and Chemistry China Academy of Engineering Physics for performing irradiation work. This work was supported by National Natural Science Foundation of China Grant Nos. 11575090 and 11605099.

## References

[1] S. Liu, Y. Bai, H. Chen, C. Li, Q. Huang, Y. Wu, F.D.S. Team, Chin. J. Nucl. Sci. Eng. 29 (2009) 266.
[2] J. Han, Y. Chen, X. Ma, S. Yang, R.A. Forrest, At. Energy Sci. Eng. 43 (2009) 389.
[3] Y. Mu, H. Xu, Z. Xiang, Y. Li, S. Wang, J. Liu, High Energy Phys Nucl. Phys. 19 (1991) 66–70.
[4] J. Luo, J. Han, R. Liu, L. Jiang, Z. Liu, G. Sun, S. Ge, Radiat. Phys. Chem. 86 (2013) 79–83.
[5] Y. Zhang, J. Xu, L. Wu, Y. Zheng, L. Bai, P. Liu, Z. Yang, Y. Xie, J. Sichuan Univ. 36 (1999) 244–246.
[6] Experimental Nuclear Reaction Data (Database Version of June 29, 2018), IAEA Nuclear Data Services. < https://www-nds.iaea.org/ > .
[7] Evaluated Nuclear Data File (Database Version of April 20, 2018), IAEA Nuclear Data Services. < https://www-nds.iaea.org/ > .
[8] ROSFOND-2010 (Russia, 2010), Russia evaluated neutron data library, issued in 2010. < https://www-nds.iaea.org/exfor/servlet/E4sGetTabSect?SectID=1245131&req=1826&PenSectID=6942460 > .
[9] ENDF/B-VII.0 (USA, 2006), U.S. evaluated neutron data library, issued in 2006. < https://www-nds.iaea.org/exfor/servlet/E4sGetTabSect?SectID=238455&req=1828&PenSectID=7611486 > .
[10] ENDF/B-VIII.0 (USA, 2018), U.S. evaluated neutron data library, issued in 2018. < https://www-nds.iaea.org/exfor/servlet/E4sGetTabSect?SectID=9009454&req=1828&PenSectID=13647465 > .
[11] JEFF-3.3 (Europe, 2017), evaluated nuclear data library of the OECD Nuclear Energy Agency. < https://www-nds.iaea.org/exfor/servlet/E4sGetTabSect?SectID=9121318&req=1828&PenSectID=13759872 > .
[12] JENDL-4.0 (Japan, 2012), Japanese evaluated neutron data library 2010 + update of 2012. < https://www-nds.iaea.org/exfor/servlet/E4sGetTabSect?SectID=1278636&req=1828&PenSectID=6846316 > .
[13] CENDL-3.1 (China, 2009), Chinese evaluated neutron data library, issued in 2009. < https://www-nds.iaea.org/exfor/servlet/E4sGetTabSect?SectID=1209023&req=1828&PenSectID=6523325 > .
[14] A.Koning, S. Hilaire, S. Goriely. User Manual of Talys-1.8,2015. < http://www.talys.eu/download-talys/ > .
[15] M.M. Rahman, S.M. Qaim, Nucl. Phys. A 435 (1985) 43.
[16] M. Bostan, S.M. Qaim, Phys. Rev. C 49 (1994) 266.
[17] F. Cserpák, S. Sudár, J. Csika, S.M. Qaim, Phys. Rev. C 49 (1994) 1525.
[18] C.D. Nesaraja, S. Sudár, S.M. Qaim, Phys. Rev. C 68 (2003) 024603.
[19] V.E. Lewis, K.J. Zieba, Nucl. Instr. Meth. 174 (1980) 141–144.
[20] NuDat 2.6 (selected evaluated nuclear structure data, Decay Radiation database version of 5/18/2017, IAEA Nuclear Data Services. < https://www-nds.iaea.org/ > .
[21] R.B. Firestone, V.S. Shirley, Table of Isotopes, Wiley, New York, 1996.
[22] X. Kong, R. Wang, Y. Wang, J. Yang, Appl. Radiat. Isot. 50 (1999) 361–364.
[23] M. Wagner, H. Vonach, A. Pavlik, B. Strohmaier, S. Tagesen, J. Martinez-Rico, Evaluation of cross sections for 14 important neutron-dosimetry reactions, Physik Daten-Phys. Data 13 (1990) 183.
[24] A.J. Koning, D. Rochman, Modern nuclear data evaluation with the TALYS code system, Nucl. Data Sheets 113 (2012) 2841–2934.
[25] A.J. Koning, J.P. Delaroche, Local and global nucleon optical models from 1 keV to 200 MeV, Nucl. Phys. A 713 (2003) 231–310.
[26] J. Raynal. Notes on ECIS94, CEA Saclay Report No. CEAN-2772, 1994.